MULTIDISCIPLINARY DESIGN OPTIMIZATION OF ADVANCED AIRCRAFT CONFIGURATIONS

A. A. Giunta, O. Golividov, D. L. Knill
B. Grossman, R. T. Haftka, W. H. Mason, L. T. Watson

MAD Center Report 96-06-01

Multidisciplinary Analysis and Design Center for Advanced Vehicles
Virginia Polytechnic Institute & State University
Blacksburg, VA 24061-0203

(540) 231-6611, grossman@aoe.vt.edu

Keynote paper presented by B. Grossman at the *15th International Conference on Numerical Methods in Fluid Dynamics*, Monterey, CA, June 26, 1996, *Lecture Notes in Physics, 490*, Eds: P. Kutler, J. Flores, J.-J. Chattot, Springer-Verlag, pp. 14–34.

MULTIDISCIPLINARY DESIGN OPTIMIZATION OF ADVANCED AIRCRAFT CONFIGURATIONS

A. A. Giunta, O. Golividov, D. L. Knill
B. Grossman, W. H. Mason, L. T. Watson
Virginia Polytechnic Inst. & State Univ., Blacksburg, VA 24061, USA
(540) 231-6611, grossman@aoe.vt.edu
and
R. T. Haftka
University of Florida, Gainesville, Florida 32611, USA

1. Introduction

Multidisciplinary design optimization (MDO) has received considerable attention in the aircraft industry, Ref. 1, as manufacturers employ concurrent engineering design practices in an effort to reduce the time-to-market of new products. While there are several computer programs which perform conceptual-level aircraft MDO, *e.g.*, Ref. 2, aircraft *system* MDO at the more advanced preliminary and detailed level of design remains computationally intractable. There has been considerable progress in single discipline design methods at the detailed level, *e.g.*, Refs. 3–6 for aerodynamic design involving Euler/Navier-Stokes solutions and there is heightened interest in the two discipline MDO problem coupling concurrent aerodynamic and structural evaluations via Euler/Navier-Stokes and finite element analyses, *e.g.*, Ref. 7. The detailed-level aircraft system MDO, however, remains unsolved, mainly because of the computational challenges brought on by the large number of constraints which must be imposed requiring detailed analyses not only at the design conditions but also throughout the flight envelope, including detailed performance evaluations, stability and control requirements during takeoff and landing and large numbers of load conditions required for structural design. Our group has been addressing some of these issues over the past decade in a sequence of example design problems of increasing levels of sophistication, Refs. 8–10. We have developed two strategies for dealing with the computational issues in MDO systems design. The first is what we term *variable-complexity modeling*, whereby we simultaneously utilize computational models of different levels of fidelity to reduce the computational effort. The MDO process is performed using low level models which are periodically corrected using higher-level models in a sequential approximate optimization. This approach as applied to High-Speed Civil Transport (HSCT) design, Refs. 9 and 10, is effective in reducing the computational costs of MDO. However, a number of problems remain. This strategy does not appear to be entirely adequate to include detailed-analysis-level CFD/Structures in a system MDO. Furthermore we have seen problems in convergence in gradient-based optimization methods for these applications. The convergence difficulties stem from noise in various parts of the analyses, Ref. 11, and often lead to the appearance of several local optima.

Our second strategy involves the utilization of statistical techniques including design of

Keynote paper presented by B. Grossman at the *15th International Conference on Numerical Methods in Fluid Dynamics*, Monterey, CA, June 26, 1996, *Lecture Notes in Physics, 490*, Eds: P. Kutler, J. Flores, J.-J. Chattot, Springer-Verlag, pp. 14–34.

experiments (DOE), Ref. 12 and response surface (RS) methodologies, Ref. 13, in order to overcome the computational costs and numerical noise problems inherent in aircraft MDO. DOE methods can be used to establish a framework for the selection of a limited number of expensive computational experiments and to provide guidelines for the accuracy and type of information which can be gained from them. Response surface modeling can be used to produce models (surface fits) which relate the dependence of the observed responses to the values of the design variables. These methods may be used effectively in conjunction with parallel computing.

To demonstrate how DOE and RS methodologies can aid in aircraft MDO, a full factorial experimental design was used to define an initial batch of HSCT configurations which were analyzed using the most inexpensive conceptual-level analysis methods. After screening out any grossly unsuitable HSCT configurations a D-optimal experimental design was used to identify a select few of the HSCT configurations for which more expensive, detailed analyses were conducted. Response surface models were then created from this data for aerodynamic drag and structural weight. The RS models were then used in the optimization process in lieu of the computationally expensive and noisy analysis methods. Thus, the computational costs of aircraft MDO were transferred from the optimization stage to the DOE stage of aircraft design. In this strategy, coarse-grained parallel computing may be applied to efficiently perform the numerous aircraft configuration evaluations specified by the DOE methods. The parallel computing methods used in this study are detailed in Ref. 14. Some preliminary results using response surface models in a simple HSCT wing shape optimization problem appear in Ref. 15 and for a wing weight problem in Ref. 16.

In Section @ of the paper, we will discuss the computational challenges of performing aircraft system MDO, particularly in contrast to single discipline design optimization. We also describe the implementation of variable-complexity modeling. In section 3 we describe our approach to the design optimization of a supersonic transport aircraft as a testbed for the development of MDO techniques. We present details of the geometry parametrization, constraints and our analysis and optimization routines. A few sample results using our variable-complexity modeling will be described along with the positive features and drawbacks of this approach. The next section gives some results on our studies on the effects of code fidelity on design optimization. In particular, we discuss our ongoing research efforts aimed at incorporating detailed-level Euler/Navier Stokes analyses (Ref. 17) into the variable-complexity modeling method. In Section 5 we summarize our work on implementing response surfaces in the MDO process. We focus on how this approach alleviates convergence problems and local extrema associated with noise in the analysis methods. We indicate how response surfaces can be developed for large dimensional design spaces using variable-complexity models and how well-suited this approach is for parallel computation. We then have some concluding remarks on future directions for this research.

2. Aircraft MDO

2.1. Single-discipline vs. multidisciplinary design

There has been considerable progress in the development of efficient procedures for single discipline aerodynamic design. These problems are generally either inverse or direct design

problems with a few constraints. They are also single point design problems such as the determination of the aerodynamic shape to optimize performance at cruise conditions. For a relatively large problem with N shape parameters where N may be $\mathcal{O}(100)$. If we perform the optimization with numerical sensitivities, then at least $(N+1)$ analyses will be required for each iteration. If the optimizer requires M iterations to converge, where for a problem this size, M may be $\mathcal{O}(50)$, then the number of analyses needed to produce a design optimization will be $\mathcal{O}(5000)$. There are efficient means to reduce the number of analyses required to calculate the sensitivity derivatives. For example, Jameson and Reuther, Ref. 3 have effectively used adjoint methods to calculate design sensitivities at a cost which is approximately independent of the number of design variables. In the adjoint approach, at each iteration, one flow analysis and one solution to the adjoint problem is required, where the solution to the adjoint problem may be considered to be approximately the same order of computational effort as one flow analysis. Thus adjoint solutions require $\mathcal{O}(2M)$ flow analyses or for our example, $\mathcal{O}(100)$ flow analyses. Another class of problems, sometimes called *one-shot methods* have been proposed, *e.g.*, Ta'asan *et al.*, Ref. 6. In this approach the flow solution, adjoint solution and optimization are solved simultaneously. These methods offer the promise of complete design optimizations in $\mathcal{O}(2)$ analyses, however, only very limited cases have been solved so far.

A relatively straightforward MDO problem which has been of recent interest is aerodynamic-structures system design. The problem is generally stated as the design of the aerodynamic shape and structural sizes for a specific mission to minimize take-off weight. In order to estimate the amount of computational effort required we consider N configuration shape parameters, with again N of $\mathcal{O}(100)$ and L structural sizing parameters, with L of $\mathcal{O}(100)$. Calculating numerical design sensitivities will require $(N+1)$ flow analyses and $(N+L+1)$ structural analyses per iteration. Note that the structural geometry and loads are affected by the aerodynamic design variables. Furthermore the structural optimization is not performed at the design conditions but is evaluated at off-design conditions. An intermediate level design will require the consideration of multiple load cases, perhaps of $\mathcal{O}(50)$ aerodynamic loads, each requiring a flow analysis. All of this must be performed in an optimization loop which may require $\mathcal{O}(50)$ iterations. We may note that adjoint methods will not be effective for MDO problems which require the transfer of large amounts of information from one discipline to the other, *e.g.*, sensitivity of structural weight with respect to aerodynamic design variables.

The situation will be further complicated by the large number of constraints which must be satisfied. There will be performance constraints at cruise, such as a constraint on the aircraft range. This will require an integration of the drag throughout the flight envelope, which may require as many as $\mathcal{O}(100)$ aerodynamic analyses at each step of the optimization. There will also be performance constraints at take-off and landing. These constraints will require low-speed aerodynamic analyses to determine the stability and control derivatives C_{L_α}, C_{M_α}, C_{M_δ} along with their design sensitivities. The structural optimization also requires a large number of local constraints on stress, strain and buckling, to be satisfied.

Thus we may roughly estimate that a single discipline aerodynamic design may require

$\mathcal{O}(100)$ –$\mathcal{O}(1000)$ analyses, whereas a multi-disciplinary systems design is considerably more complex and may require $\mathcal{O}(10,000)$ – $\mathcal{O}(100,000)$ analyses. Considering the computational expense involved in high-fidelity aerodynamic and structural analyses, it appears that using a brute-force optimization with black-box aerodynamic and structural codes is not practical in the foreseeable future. Instead, one must look for clever formulations to perform aircraft systems MDO which significantly reduce the computational burden. This has been the motivation of our research group for the past 12 years and forms the objective of the work presented here.

2.2. Variable-complexity modeling

A growing practice in MDO is the use of approximation associated with what we term variable-complexity modeling (VCM). For example, the structural design of an aircraft is often performed with a complex structural model, but with loads obtained from simple aerodynamic models. Similarly, the aerodynamic designer may use advanced aerodynamic models with a simple structural model to account for wing flexibility effects.

We have employed a VCM approach using both the simple and complex models during the optimization procedure. Our aim is to take advantage of the low computational cost of the simpler models while improving their accuracy with periodic use of the more sophisticated models. The sophisticated models provide scale factors for correcting the simpler models. These scale factors are updated periodically during the design process. For example, in Ref. 10 we combined the use of simple and complex aerodynamic models to predict the drag of an HSCT during the optimization process. Similarly, in Ref. 18 we employed structural optimization together with a simple weight equation to predict wing structural weight in combined aerodynamic and structural optimization of the HSCT. We have also used this approach to handle the estimation of stability and control derivatives, Ref. 19.

The variable-complexity modeling approach is used within a sequential approximate optimization technique whereby the overall design process is composed of a sequence of optimization cycles. At the beginning of each cycle, approximations are constructed using either scaled, global-local or interlacing approximations.

The scaled approximation, which employs a constant scaling function σ, given as

$$\sigma(\mathbf{x_0}) = \frac{f_d(\mathbf{x_0})}{f_s(\mathbf{x_0})}, \tag{1}$$

where f_d represents a detailed model analysis result, and f_s represents a simple model analysis result, both evaluated at a specified design point, $\mathbf{x_0}$, at the beginning of an optimization cycle. During an optimization cycle the scaled approximate analysis results, $f(\mathbf{x})$, are calculated as

$$f(\mathbf{x}) \approx \sigma(\mathbf{x_0}) f_s(\mathbf{x}). \tag{2}$$

Thus, the scaled simple analysis is used throughout the cycle until convergence. Then a new value of the scale factor is computed and the optimization is repeated. Move limits are imposed during the optimization cycles.

Other approaches that we have utilized in Refs. 10 and 18 include what we term a global-local approximation which involves estimating the derivatives of the scale factor. For more expensive analyses the scaled approximation is used, but with the scale factor updated only every fifth cycle. This procedure, called interlacing, has been used for estimating structural weight, Ref 18. The implementation of the VCM approach in an MDO problem for the design of a high-speed civil transport is described next.

3. High-Speed Civil Transport Testbed

The design optimization of the configuration for the next-generation supersonic transport aircraft called the high-speed civil transport (HSCT), Fig. 1, serves as an effective testbed for the development of MDO methodology. We consider the design problem to be the minimization of the takeoff gross weight (TOGW) of a 250 passenger HSCT with a range of 5,500 nautical miles and a cruise speed of Mach 2.4.

The HSCT external configuration and mission are defined using 29 variables listed in Table 1. Twenty-six of these variables describe the geometric layout of the HSCT and three variables describe the mission profile. The airfoil and planform variables are shown in Figure 2. In this parametrization, eight variables describe the wing planform, eight variables define the area ruled fuselage shape distribution, five variables define the airfoil section properties, two variables define the engine nacelle locations, two variables define the horizontal and vertical tail areas, and one variable defines engine thrust. For this HSCT design problem the fuselage has a fixed length of 300 ft and an internal volume of 23,720 ft^3. More details of the configuration parametrization are in Ref. 10.

The idealized mission profile is divided into three segments: takeoff, supersonic cruise/climb at Mach 2.4, and landing. The three mission design variables are fuel weight, starting altitude for the supersonic cruise/climb segment, and rate-of-climb during the supersonic cruise/climb segment. If the HSCT reaches the maximum ceiling of 70,000 ft, supersonic cruise at Mach 2.4 is maintained at that altitude for the duration of the supersonic mission leg.

Our HSCT design employs 69 nonlinear inequality constraints which consist of both geometric constraints (e.g., all wing chords $\geq 7.0ft$), and aerodynamic/performance constraints (e.g., C_L at landing ≤ 1, and range $\geq$ 5,500 $naut.mi.$). These are listed in Table 2. A discussion of these constraints may be found in Refs. 18 and 19.

The HSCT design objective is to minimize TOGW, where TOGW is a nonlinear, implicit function of the 29 design variables. In formal optimization terms this problem may be expressed as

$$\begin{aligned} &\min_{\hat{x} \in R^{29}} TOGW(\hat{x}) \\ &\text{subject to } g_i(\hat{x}) \leq 0, \qquad i = 1, \ldots, 69, \end{aligned} \tag{3}$$

where $\hat{x}$ is the 29-dimensional vector of design variables, and $g(\hat{x})$ is the 69-dimensional vector of nonlinear inequality constraints.

The take-off gross weight may be written as

$$TOGW = W_{payload} + W_{fuel} + W_{structural} + W_{non-structural}\,, \tag{4}$$

where the payload weight is fixed and the fuel weight is a design variable determined by the optimization process. As a first approximation we may estimate the aircraft structural and non-structural weight from a set of algebraic weight formulas given in FLOPS, Ref. 2. However, based on detailed studies in Ref. 20, the structural weight of the wing may not be adequately estimated using the FLOPS weight equations. Within our variable-complexity framework, we have also implemented a crudely modeled finite-element model for the wing structure using 923 elements, with 193 nodes and 579 degrees of freedom. The structural optimization uses 5 load cases, and consider 40 design variables involving 26 groupings of skin thickness, 12 spar cap areas and 2 rib cap areas to model one half of the wing. Details of the geometry modeling and structural optimization appear in Ref 20. A plot of the internal wing geometry and the finite-element model appear in Fig. 3.

For these efforts we have developed a suite of conceptual-level or *simple* analysis methods and preliminary-level or *detailed* analysis tools which we utilize within the context of variable-complexity modeling, Eq. (1). The conceptual level tools consist of mainly in-house codes described in Ref. 18 involving various algebraic and simplified analysis methods for supersonic cruise, low-speed performance including stability derivatives for take-off and landing constraints. At this level, the weight is estimated using the algebraic relationships given in FLOPS, Ref. 2. The detailed analysis tools, also described in Ref. 18, include the Harris wave drag code, Ref. 21, the supersonic panel code WINGDES, Ref. 22, a subsonic vortex lattice code and an approximate viscous drag routine. Some details of these codes are also discussed in Ref. 18. In addition we have investigated the effects of including Euler and Navier-Stokes analyses in the design process, Ref. 17, using the code GASP, Ref. 23. At the detailed level, structural optimization may be included for the material bending weight of the wing through the code GENESIS, Ref. 24. The numerical optimization software is an extended exterior penalty function code NEWSUMT-A, Ref. 25 and a sequential quadratic programming (SQP) method in code DOT, Ref 26. Figure 4 is a flowchart which shows how the analysis and optimization tools are coupled to perform HSCT design optimization.

We have performed MDO for several related HSCT designs. The most complete description of the cases considered appears in Ref. 27. Cases are considered for a wing-fuselage design (with a fixed vertical tail), a wing-body-vertical tail design and a complete wing-body with vertical and horizontal tail. The latter design is performed with and without the engine thrust as a design variable, with different balanced field length constraints and with and without a subsonic leg in the mission profile.

We present here one sample result from that report, which we call design 29c. This is a design which includes all of our options except for the subsonic leg portion of the flight envelope. Some of the design parameters calculated for this case are listed in Table 3, along with their initial values. The initial and final planform for this case appear in Fig. 5. For this case the initial data did not satisfy a number of constraints, most notably the range constraint. The tabulated data indicates that the final design required additional weight to satisfy this and other constraints. The final design required higher engine thrust, a heavier propulsion system weight and had minor planform changes including moving the nacelles inboard.

The main purpose of including a sample design result here is to discuss the convergence of this procedure. In Fig. 6, we give plots of the takeoff gross weight, TOGW and the range versus iteration number. Note that each iteration is a cycle within a sequential approximate optimization and consists of a converged design using the simple (algebraic) analyses which are multiplied by a constant scale factor. At the end of each cycle the scale factor is updated from a detailed analysis and the process repeated. We have found that this process takes typically from 40 to 70 iterations to converge, with the latter value needed for the sample case in Fig. 6.

We have investigated this process and determined that the slow convergence can usually be traced to analyses which have a noisy response to small changes in design parameters. We have found this to occur with our panel-level detailed supersonic aerodynamic analysis codes, Ref. 15, with structural weight computed from structural optimization, Ref. 16 and from results from CFD analyses, Ref. 28. A typical variation is shown in Fig. 7 where the wave drag is plotted for a wing for different values of the wing semi-span. We see a high frequency *noise* in the analysis with an amplitude of the order of one tenth of a count of drag. For a single analysis, this degree of variation is inconsequential, with accuracy on the order of one count of drag generally expected. However, this variation can cause difficulties within an optimization process, where sensitivity derivatives of quantities such as drag with respect to geometric design parameters are required. The noise in the sensitivity derivatives leads to slow convergence and even to local *extrema* in the design space. These local *extrema* were discussed in Refs. 11, 18 and an example will be presented here in Section 5.

Overall the variable-complexity modeling approach outlined here has been very successful in reducing the computational burden of MDO aircraft design. A typical approximate cycle uses about 750 simple analyses, and one detailed analysis for a scaled approximation. Overall, 40–70 approximate cycles are required for global convergence. Since the computational cost associated with the simple models was at least 50 times smaller than the cost of the detailed model, very considerable savings are realized using variable-complexity modeling. However, this type of cost-saving is not adequate to include the most detailed analysis methods in the MDO process. In the next section we will discuss some of the implications of including detailed Navier-Stokes analyses in the design optimization. In Section 5, we will discuss a procedure which will allow us to include higher fidelity analyses and to avoid some of the problems associated with noisy analysis procedures.

4. Effects of Code Fidelity on Design Optimization

The aerodynamics used in our HSCT design study involved methods based on panel-level codes including vortex-lattice methods for low speed performance and supersonic-panel codes, Ref. 22 and slender-body theory, Ref. 21 for high-speed performance. In Ref. 17, we have performed verification, validation and certification of an Euler and Navier-Stokes code for HSCT aerodynamic calculations. We have used the code GASP, Ref. 23 for this purpose.

A careful grid convergence study was for HSCT wings and wing-body combinations was performed for both Euler and Navier-Stokes grids. Examples of drag convergence versus

the number of grid points is shown in Fig. 8 for the Euler solution and in Fig. 9 for the Navier-Stokes solution. A plot of the drag polar for an HSCT wing-body at $M = 2.4$ is presented in Fig. 10. Results from a PNS calculation along with the Euler results with a boundary layer correction and the results from the linear supersonic methods which also have a boundary layer correction are compared in the figure. At a cruise $C_L = .082$ the values of C_D are given in Table 4. We find that there is about a 2 count difference between the boundary-layer corrected Euler and the Navier-Stokes solutions and an additional 2 count discrepancy between the Euler and linear theory solutions.

These small differences in drag lead to substantial differences when integrated to give the aircraft range. As given in Table 4, the computed aircraft range values for the three computation methods presented resulted in range values of 5197, 5367 and 5495 nautical miles, with the smallest value the PNS result and the largest value the linear theory result. Since the range is always an active constraint on the HSCT design optimization, it was surmised that the code fidelity could have a large effect on the MDO results. To verify this we recomputed our HSCT design optimization, with the parametric addition and subtraction of up to 2 counts of drag. Results of this study are presented in Fig. 11 which gives the optimized $TOGW$ plotted versus the arbitrary drag increment. We see that the optimized weight can change from a baseline value of $800,000$ $lbs.$ to a value of $820,000$ $lbs.$ with a $+2$ count drag increase and to a value of $740,000$ $lbs.$ with a -2 count drag decrease. The effect of these drag changes on the geometric planforms are shown in Figs. 12 and 13 with details presented in Ref. 27.

It was also observed that the wing loading distributions were considerably different for the PNS, Euler and linear theory cases. The structural optimization was then performed with both the Euler and linear theory loads. Although the differing loads produced a varying stress distributions, the optimized weights showed minimal effects, with wing bending material weights agreeing to within 3% as shown in Table 4.

Our initial exploration of code fidelity on the design optimization of the HSCT in Ref. 12 appears to show a strong sensitivity to the accuracy of the range calculation. The effect on the computed loads appears to be much smaller for the structural optimization. However, we need to perform a more thorough study, particularly for transonic loads. The cost of increasing code fidelity in a system-level MDO is enormous. For example, on an SGI Power Challenge XL, a single analysis of our linear theory analysis takes between 1 and 2 seconds, the Euler analysis takes 15–20 minutes and the PNS solution takes 1.25–3 hours. Clearly the previous variable-complexity modeling approach is not adequate to effectively handle higher fidelity codes. This motivated our group to consider using response surfaces, which are particularly well-suited to be used in conjunction with coarse-grained parallel computing as a means of addressing computational costs.

5. Response Surface Approach

We have described some of the difficulties associated with systems level aircraft MDO. One issue is the huge computational burden associated with the very large numbers of detailed analyses required in the MDO process. Our approach called variable-complexity modeling was somewhat successful at reducing the computational expense, but still was

not adequate to allow the implementation of the highest level of fidelity analyses in the optimization process. In addition we have pointed out that many of the analysis codes have levels of noise which make the evaluation of accurate sensitivity derivatives difficult or impossible to obtain. This was seen to lead to slow convergence and a design space filled with local extrema.

Another issue that we have encountered is the complexity of *software engineering* with this approach. We have had to accumulate a large number of *black box* codes, for aerodynamics, structures, performance, propulsion, stability and control and optimization into a single code. This task was very difficult to accomplish in a research environment. Some of the issues that created software integration problems include: code components were written in different languages including non-standard ones, new code components required new interfaces, MDO practitioners have only limited knowledge about disciplinary components and optimizers, changes and updates to components affect the entire code, code components became obsolete due to changes in computer systems and, in general, code components were written for analysis, not optimization. This led to an ever growing share of our time being devoted to code maintenance, along with poor reliability of the MDO code and portability problems.

Our approach to these difficulties is influenced by traditional design approaches, used before the introduction of high speed computers. An examination of the process of traditional aircraft design reveals that aircraft designers faced a very similar dilemma to the one we encountered. The analysis tools available forty years ago were computationally inexpensive, but often required specialized expertise beyond what could be expected of the generalists who practiced the art of aircraft design. Therefore the analysis tools were extensively exercised by their own developers to produce design charts and carpet plots which could be directly used by designers. That is, when a researcher developed a new method, he normally produced copious tables and charts, which permitted designers to benefit from the new capability without needing to master the new technique. Additionally, experimental results complemented the analytically generated charts, or were used to generate charts of correction factors to be applied to the analytically generated charts. This process of giving the designer the *results* of the analysis tools rather than the *tools* themselves is somewhat limited in that design charts and tables are manageable only when the response is a function of a small number of variables. To reduce the number of parameters appearing in design charts, researchers put a lot of effort into compressing results with the aid of nondimensional similarity parameters. The same approach is used to this day in reporting experimental results. Many experimentalists strive to discover combinations of variables that will allow them to collapse a large number of experimental observations into a small number of graphs. This process also filters out much of the noise due to experimental errors.

We are in the process of developing a similar approach to solve our problem of integration of analysis software. This approach is based on response surface methods and variable complexity modeling in a combination we call variable-complexity response surface modeling, VCRSM. Response surface modeling (RSM) is a collection of techniques for approximating functions based on their values at a number of points. Usually the approximation takes

the form of a low-order polynomial, however, even neural networks can be viewed as a special case of response surface approximations. RSM can be used to re-introduce the traditional design paradigm of giving designers the results of analysis tools rather than the tools themselves.

This can be accomplished by running a large number of analyses for different sets of inputs on each analysis code. Then, the results are fitted by a response surface (*e.g.*, quadratic polynomial) in terms of the input variables, and the designer is given the response surface instead of the analysis code. With the RS being a simple formula instead of a design chart, the limit of 2 or 3 variables is removed, so that in theory any number of variables can be used. Additionally, the creation of the RS, which is essentially a curve-fitting operation, can be used to filter out noise in the data.

This approach does not require tying an optimizer to analysis programs because the optimizer operates on the RS rather than the original data. RS techniques are therefore well suited for working with *black-box codes* that cannot be incorporated easily into larger systems. The approach also respects *organizational boundaries* in that response surfaces can be generated by various organizations using their preferred computer codes on their own computers. Finally, with the large number of analyses that need to be executed for sets of predetermined data points, maximum use can be made of parallel computation with minimal need to change codes to take advantage of parallelization.

Unfortunately, when the number of variables associated with the response surface becomes large, we encounter the so-called *curse of dimensionality*. Even with quadratic polynomials the number of coefficients increases as the square of the number of variables. The number of analyses required to evaluate these coefficients increases in a similar manner. Furthermore, often the accuracy of the response surface deteriorates with increasing dimensionality. Therefore, the brute-force application of response surfaces to aircraft design is useful only when the number of variables defining the design is small, typically less than 10. When the number of variables is larger, a more intelligent use of RS techniques is warranted.

To combat the loss of accuracy associated with high dimensionality we customize the response surface to a small region in design space tailored to a specialized design problem. For example, while old design charts provide drag coefficients for what was considered to be all likely planforms, we need information only for planforms which are reasonable for a particular flight Mach number. In that way we imitate traditional designers. Unlike modern optimization programs, traditional designers did not waste time analyzing designs which are patently nonsensical.

To limit the design space we employ the simpler analysis tools of the previous generation of designers, tools which have lower accuracy than their modern counterparts, but which require only minuscule amount of computation on present-day computers. These tools may not be accurate enough to identify optimal or near optimal designs. However, they can identify vast regions in design space which correspond to *nonsense* designs that should not be analyzed by more expensive modern techniques.

We have been working on response surfaces for several components of our HSCT code.

The following description of the construction of a response surface for evaluating supersonic cruise drag from Ref. 29 illustrates the principles of VCRSM. A description of this approach applied to developing a response surface for structural weight appears in Refs. 16 and 30. A description of the strong compatibility of this approach with parallel computing appears in Ref. 14.

Experimental design theory, Ref. 12, is a branch of statistics which provides the researcher with numerous methods for selecting the independent variable values at which a limited number of experiments will be conducted. The various experimental design methods create certain combinations of numerical experiments (analyses) in which the independent variables are prescribed at specific values or *levels.* The results of these planned experiments are used to investigate the sensitivity of some dependent quantity, identified as the *response,* to the independent variables. Other statistical techniques known as regression analysis and analysis of variance (ANOVA) are employed in the response sensitivity investigation. They are used to perform a systematic decomposition of the variability in the observed response values and to assign portions of the variability to either the effect of an independent variable or to experimental error. In using ANOVA with numerical experiments, numerical noise takes the place of experimental error.

RSM is a formal process combining elements of experimental design, regression analysis, and ANOVA, Ref. 13. RSM employs these statistical methods to create functions, typically polynomials, to model the response or outcome of a numerical experiment in terms of several independent variables, e.g., wave drag expressed as a function of several wing planform variables. In many RSM applications, either linear or quadratic polynomials are assumed to accurately model the selected response. Although this is certainly not true for all cases, RSM becomes prohibitively expensive when cubic and higher-order polynomials are chosen for experiments involving several variables. Giunta *et al.*, Ref. 11, concluded that quadratic polynomial models were sufficiently accurate for HSCT configuration design.

A quadratic response surface model has the form

$$y = c_o + \sum_{1 \le j \le m} c_j x_j + \sum_{1 \le j \le k \le m} c_{jk} x_j x_k, \tag{5}$$

where y is the response, x_j represents the m design variables, and c_o, c_j, and c_{jk} are the unknown polynomial coefficients. Note that there are $n = (m+1)(m+2)/2$ coefficients in this quadratic polynomial. To estimate the unknown polynomial coefficients in the RS model, at least p response values must be available, where $p \ge n$. Under such conditions, the estimation problem may be formulated in matrix notation as $Y \approx \mathbf{X}c$, where Y is the p by 1 vector of observed response values, $\mathbf{X}$ is a p by n matrix of constants assumed to have rank n, and c is the n by 1 vector of unknown coefficients to be estimated. The least squares solution to $Y \approx \mathbf{X}c$ is $\hat{c} = (\mathbf{X}^T\mathbf{X})^{-1}\mathbf{X}^T Y$. Typically values for p of at least $1.5n$ to $2.5n$ are required to produce response surface models which accurately model the trends in the calculated data, Ref. 11. A discussion on using statistical methods to measure the effectiveness of response surface fits is discussed in Ref. 29.

The problem of selecting the design variables where the analysis will be performed in order to perform the response surface fit is called the experimental design. In Ref. 29, we describe

two methods, full factorial design and D-optimal design. Prior to experimental design, the allowable range of each of the m variables is defined by lower and upper bounds. The allowable range is then discretized at equally-spaced levels. For numerical stability and for ease of notation the range of each variable is scaled to span $(-1, 1)$, Ref. 13. The region enclosed by the lower and upper bounds on the variables is termed the *design space,* the vertices of which determine an $m-$dimensional cube or *hypercube.* If each of the variables is specified at only the lower and upper bounds (two levels), the experimental design is called a 2^m full factorial. Similarly, a 3^m full factorial design is created by specifying the lower bound, midpoint, and upper bound (three levels) for each of the m variables.

The construction of a quadratic response surface model in m variables requires at least $n = (m + 1)(m + 2)/2$ response evaluations. A 3^m full factorial design provides ample response evaluations to permit the estimation of the RS model coefficients. For example, fitting a quadratic response surface model in three variables ($m = 3$) requires at least ten evaluations, and a 3^3 full factorial design provides 27 evaluations. However, as m becomes large the evaluation of both 2^m and 3^m full factorial designs becomes impractical (e.g., 2^{10} =1,024 and 3^{10} =59,049). A full factorial design typically is used for ten or fewer variables.

RSM typically employs a full factorial or similar experimental design. However, full factorial designs are intended for use with rectangular design spaces and not the irregularly shaped (even nonconvex) design spaces that may arise in the HSCT design problems considered here. Previous studies, Refs. 11, 15, found that the D-optimality criterion, Ref. 13, provides a rational means for creating experimental designs inside an irregularly shaped design space.

The objective of the D-optimality criterion is to select the set of p locations in a design space from a pool of q candidate locations ($q \geq p$), such that the quantity $|\mathbf{X}^T\mathbf{X}|$ is maximized. Note that the pool of q candidate locations is defined *a priori* by the user, and the p locations which maximize $|\mathbf{X}^T\mathbf{X}|$ are found iteratively using a numerical optimization method. The set of p locations for which $|\mathbf{X}^T\mathbf{X}|$ is maximum is called a D-optimal experimental design. The statistical reasoning behind the creation of a D-optimal design is that it leads to response surface models for which the maximum variance of the predicted responses is minimized. In non-statistical terms, the D-optimality criterion ensures that the p locations are selected at points in the design space which will minimize the error in the estimated coefficients, $\hat{c}$, in the response surface model. A discussion of several methods to create D-optimal experimental designs is given in Ref. 29.

The construction of the response surface models may be viewed as a series of steps to be completed before the aircraft system optimization is performed. We call this methodology, which takes advantage of the computational savings of using both simple analysis methods and detailed analysis methods, variable-complexity response surface modeling, VCRSM. Starting from an initial HSCT configuration, a very large number of candidate designs, (20,000 in Ref. 29 and 50,000 in Ref. 30), are selected with the initial HSCT at the center of the design space. These may comprise a full-factorial design, Ref. 29, or a subset of a full-factorial design as implemented in Refs. 16 and 30, which is appropriate for designs

with more than 10 parameters. These design points are evaluated using the computationally inexpensive conceptual level analysis tools, and the HSCT analyses are screened to eliminate any grossly infeasible HSCT configurations from consideration. Next, the D-optimality criterion is applied to select a subset of the remaining HSCT configurations for evaluation using the preliminary level analysis tools. Response surface models for the aerodynamic quantities are then constructed using the preliminary level analysis data. In the final step of the VCRSM method the response surface models are used in the HSCT optimization software to replace the noise producing aerodynamic analysis methods. Thus, optimization is conducted without the problems associated with numerical noise.

We illustrate the effectiveness of the VCRSM approach with a simplified five variable HSCT wing design problem. This five variable problem is based on the 29 variable HSCT MDO problem described in Section 3. The five variables are wing root chord (C_{root}), wing tip chord (C_{tip}), thickness-to-chord ratio ($t/c\ ratio$), inboard leading edge sweep angle (Λ_{LE_I}), and fuel weight (W_{fuel}). All the remaining (24) design variables are kept fixed at baseline values. The mission profile and constraints are simplified resulting in 42 constraints applied to the example 5 design variable problem. Complete details are given in Ref. 29.

We performed design optimization for this problem with the variable-complexity response surface methodology used for all components of the drag. For comparison we also used the VCM approach described in Section 3, which did not involve response surfaces. We performed each design optimization starting from 3 different initial conditions. The results are tabulated in Table 4. The optimized planforms for the three cases without the response surface are plotted in Figs. 13 a, b and c. The optimized planforms for the three cases with the response surfaces are plotted in Figs. 14 a, b and c. The cases optimized without the response surfaces clearly result in 3 different minimum weights, 636057, 636559 and 647035 *lbs.*, respectively. The cases optimized with the response surfaces all converged to the identical value of 622804 *lbs.*

From this simple example we see that VCRSM was effective in addressing convergence issues associated with noisy analyses. Computational cost of this procedure was greatly alleviated through the use of parallel computing. Since the points in design space which are used to establish the response surface are determined *a priori*, coarse-grained parallelization is easy to implement on a distributed memory parallel system. We have utilized 28 and 100 node Intel Paragon computers and have achieved parallel efficiencies on the order of 90%, see Ref. 13. Using a *master-slave* paradigm, a coarse-grained parallelization is effectively obtained, provided that the analysis has minimal internal input/output, Ref. 14. Applications of this approach for 10 design variables also is described in Ref. 29. Plans are underway to solve the complete 29 variable HSCT problem using response surfaces. In addition this approach has been applied using weight equations and finite-element structural optimization in Refs. 16 and 30.

6. Concluding Remarks

In this paper we have expounded our view that aircraft systems MDO is computationally challenging and that at this time it is impractical to link the highest fidelity codes representing each discipline directly to an optimizer to perform MDO. We have established a

somewhat restricted HSCT design model problem as an effective testbed for MDO research. For HSCT design we have shown that variable-complexity modeling can be effective in reducing the computational burden of MDO. We have also found that aerodynamic code fidelity can have a pronounced effect on HSCT design results.

Furthermore, we have established that a response surface approach is well suited for MDO. In particular we have seen that response surface methods are appropriate to take advantage of coarse-grained parallel computing. We have realized many advantages of RSM, including the alleviation of problems associated with computational noise and the mitigation of software issues associated with coupling disparate codes from different disciplines. Response surfaces result in simplified MDO code integration which may lead to better optimization procedures including global optimization, multicriterion optimization and reliability based optimization.

However, we have still not reached our goal of performing aircraft systems level MDO with high-fidelity analysis codes. In order to achieve this goal we envision the need for a formulation which incorporates: $\mathcal{O}(10)$–$\mathcal{O}(100)$ of the highest fidelity analyses including Navier-Stokes aerodynamics, detailed finite-element structures, and perhaps even some experimental data; along with $\mathcal{O}(100)$–$\mathcal{O}(1000)$ mid-level analyses including Euler methods, panel codes, elementary finite-element structures, beam models; along with $\mathcal{O}(10,000)$–$\mathcal{O}(100,000)$ low-level analyses which are mainly algebraic or data bases models. We are currently exploring the applicability of formulations based on Bayesian statistics, *e.g.,* Ref. 31 to accomplish this task.

7. Acknowledgments

This research was partially supported by NASA Langley Research Center grants NAG1-1160 and NAG1-1562.

8. References

1. J. Sobieszczanski-Sobieski and R. T. Haftka: AIAA 96–0711, (1996).
2. L. A. McCullers: NASA CP–2327, 396, (1984).
3. J. Reuther and A. Jameson: AIAA 95–0123, (1995).
4. V. Korivi, A. Taylor, G. Hou, P. Newman and H. Jones: *AIAA J.,* **32**, 1319, (1994).
5. O. Baysal and M. E. Eleshaky: *AIAA J.,* **30**, 718, (1992).
6. S. Taásan, G. Kuruvila and M. D. Salas, AIAA 92–0005, (1992).
7. C. Byun and G. P. Guruswamy: AIAA 94–1487, (1994).
8. B. Grossman, Z. Gurdal, G. Strauch, W. Eppard and R. Haftka: *J. Aircraft,* **25**, 855, (1988).
9. E. Unger, M. Hutchison, R. Haftka and B. Grossman: *Intl. J. Systems Automation: Res. & Appl. (SARA),* **2**, 87, (1992).
10. M. Hutchison, E. Unger, W. Mason, B. Grossman and R. Haftka: *J.Aircraft,* **31**, 110, (1994).
11. A. Giunta, J. Dudley, R. Narducci, B. Grossman, R. Haftka, W. Mason and L. Watson: AIAA 94–4376–CP, 1117, (1994).
12. D. C. Montgomery: *Design and Analysis of Experiments,* Wiley, NY, (1976).
13. R. Myers and D. Montgomery: *Response Surface Methodology: Process and Product*

Optimization Using Designed Experiments, Wiley, NY, (1995).
14. S. Burgee, A. Giunta, V. Balabanov, B. Grossman, W. Mason, R. Narducci, R. Haftka and L. Watson: to appear in *Intl. J. Supercomputing Appl. & High Perf. Comp.,* (1996).
15. A. Giunta, R. Narducci, S. Burgee, B. Grossman, R. Haftka, W. Mason and L. Watson: AIAA 95–1886–CP, 21, (1995).
16. M. Kaufman, V. Balabanov, S. L. Burgee, A. A. Giunta, B. Grossman, R. T. Haftka W. H. Mason and L. T. Watson: *Computational Mechanics,* **18**, No. 2, 112, (1996).
17. D. Knill, V. Balabanov, B. Grossman, W. Mason and R. Haftka: AIAA 96–0330, (1996).
18. J. Dudley, X. Huang, R. T. Haftka, B. Grossman and W. H. Mason, AIAA 94–4377, (1994).
19 P. E. MacMillin, J. Dudley, W. H. Mason, B. Grossman and R. T. Haftka, AIAA 94–4381, (1994).
20. X. Huang, J. Dudley, R. T. Haftka, B. Grossman and W. H. Mason, *J. Aircraft,* **33**, No. 3, 608, (1996).
21. R. V. Harris, Jr., NASA TM X-947, (1964).
22. H. W. Carlson and K. B. Walkley, NASA CP 3808, (1984).
23. W. D. McGrory, D. C. Slack, M. P. Applebaum and R. W. Walters, *GASP Version 2.2 Users Manual*, Aerosoft Inc., Blacksburg VA, (1995).
24. *GENESIS Users Manual, Version 1.3,* Vanderplaats, Miura and Associates, Inc., Goleta, CA, (1993).
25. R. V. Grandhi, R. Thareja and R. T. Haftka, *ASME J. Mechanisms, Transmissions and Automation in Design,* vol. 107, 94, (1985).
26. *DOT Users Manual, Version 4.20,* Vanderplaats Research & Development, Inc., Colorado Springs, CO, (1995).
27. P. E. MacMillin, O. Golividov, W. H. Mason, B. Grossman and R. T. Haftka, MAD Center Report 96-07-01, Virginia Tech, Blacksburg, VA, July 1996.
28. R. Narducci, B. Grossman, M. Valorani, A. Dadone and R. T. Haftka, AIAA Paper No. 95-1648-CP, 21, (1995).
29. A. A. Giunta, V. Balabanov, M. Kaufman, B. Grossman, W. H. Mason, L. T. Watson and R. T. Haftka, AIAA Paper No. 96–4001–CP, (1996).
30. V. Balabanov, M. Kaufman, D. L. Knill, A. A. Giunta, R. T. Haftka, B. Grossman, W. H. Mason and L. T. Watson, AIAA Paper No. 96–4046–CP, (1996).
31. T. J. Mitchell, J. Sachs, W. J. Welch and H. P. Wynn, *Statistical Science*, Vol. 4, No. 4, 409, (1989).

Design Variable	Baseline Value	Configuration Parameter Description
1	181.48	Wing root chord, ft
2	155.9	LE break point, x ft
3	49.2	LE break point, y ft
4	181.6	TE break point, x ft
5	64.2	TE break point, y ft
6	169.5	LE wing tip, x ft
7	7.00	Wing tip chord, ft
8	75.9	Wing semi-span, ft
9	0.40	Chordwise max. thk. location
10	3.69	LE radius parameter
11	2.58	Airfoil t/c *ratio* at root, %
12	2.16	Airfoil t/c *ratio* at LE break, %
13	1.80	Airfoil t/c *ratio* at tip, %
14	2.20	Fuselage restraint 1, x ft
15	1.06	Fuselage restraint 1, r ft
16	12.20	Fuselage restraint 2, x ft
17	3.50	Fuselage restraint 2, r ft
18	132.46	Fuselage restraint 3, x ft
19	5.34	Fuselage restraint 3, r ft
20	248.67	Fuselage restraint 4, x ft
21	4.67	Fuselage restraint 4, r ft
22	26.23	Nacelle 1 location, ft
23	32.39	Nacelle 2 location, ft
24	697.9	Vertical tail area, ft^2
25	713.0	Horizontal tail area, ft^2
Design Variable	**Baseline Value**	**Performance Parameter Description**
26	39,000	Thrust per engine, lb
27	322,617	Mission fuel, lb
28	64,794	Starting cruise/climb altitude, ft
29	33.90	Supersonic cruise/climb rate, ft/min

Table 1. Design Parameters

Constraint Number	Geometric Constraint Description
1	Fuel volume $\leq$ 50% wing volume
2	Airfoil section spacing at $C_{tip} \geq 3.0ft$
3-20	Wing chord $\geq 7.0ft$
21	LE break $\leq$ semi-span
22	TE break $\leq$ semi-span
23	Root chord t/c *ratio* $\geq$ 1.5%
24	LE break chord t/c *ratio* $\geq$ 1.5%
25	Tip chord t/c *ratio* $\geq$ 1.5%
26-30	Fuselage restraints
31	Nacelle 1 outboard of fuselage
32	Nacelle 1 inboard of nacelle 2
33	Nacelle 2 inboard of semi-span
Constraint Number	**Aero. & Performance Constraint Description**
34	Range $\geq 5,500$ *naut.mi.*
35	C_L at landing ≤ 1
36-53	Section C_l at landing ≤ 2
54	Landing angle of attack $\leq 12°$
55-58	Engine scrape at landing
59	Wing tip scrape at landing
60	LE break scrape at landing
61	Rudder deflection $\leq 22.5°$
62	Bank angle at landing $\leq 5°$
63	Tail deflection at approach $\leq 22.5°$
64	Takeoff rotation to occur $\leq V_{min}$
65	Engine-out limit with vertical tail
66	Balanced field length $\leq$ 11,000 ft
67-69	Mission segments:
	thrust available$\geq$ thrust required

Table 2. Constraints

Design Variable	Initial	Final
Gross Weight (*lbs*)	732,741	772,981
Fuel Weight (*lbs*)	376,454	403,346
Fuel Wt / Gross Wt	51.4%	52.1%
Wing Area (ft^2)	12,612	13,191
Wing Weight (*lbs*)	103,247	113,086
Aspect Ratio	1.88	1.99
Vertical Tail Area (ft^2)	514.3	454.1
Vertical Tail Weight (*lbs*)	2,077	1,898
Nacelle 1 position, y (*ft*)	8.26	7.08
Nacelle 2 position, y (*ft*)	21.37	14.41
Horz. Tail Area (ft^2)	778.9	747.2
Horz. Tail Weight (*lbs*)	8,608	8,346
Time to rotate (*sec*)	5.07	5.27
Engine thrust (*lbs*)	46,480	49,258
Nacelle length (*ft*)	35.18	37.40
Nacelle diameter (*ft*)	6.53	6.95
Propulsion system weight (*lbs*)	77,884	82,791
Range (*n.mi.*)	5,373.5	5,502.9
Landing angle of attack	10.85°	10.58°
Balanced Field Length (*ft*)	11,094	10,922
$(L/D)_{max}$	9.132	9.155

Table 3. Sample Design Case 29c

	PNS	Euler $+C_f$	Lin. Th. $+C_f$
C_d at cruise	0.00803	0.00774	0.00753
Range, *n. mi.*	5197	5367	5495
Opt. Wing Struct. Weight, *lbs.*		22,144	22,794

Table 4. Code Fidelity Comparisons

Case	Initial Design TOGW *lbs.*	VCM Design (no resp. surf.)	VCRSM Design (resp. surf.)
a.	639,851	636,057	622,804
b.	712,961	636,559	622,804
c.	671,823	647,035	622,804

Table 5. Five Variable Design

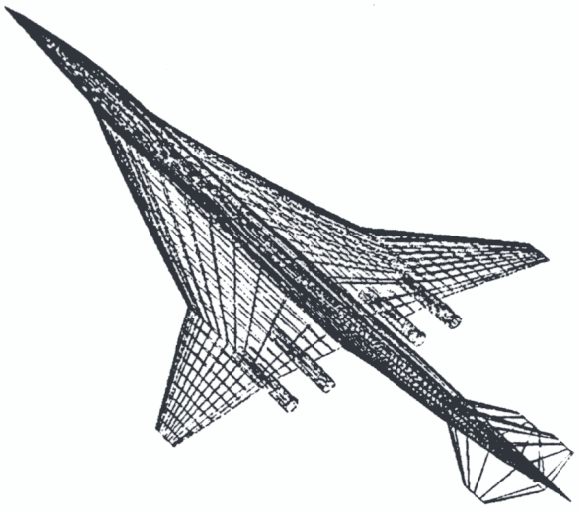

Fig. 1. HSCT configuration.

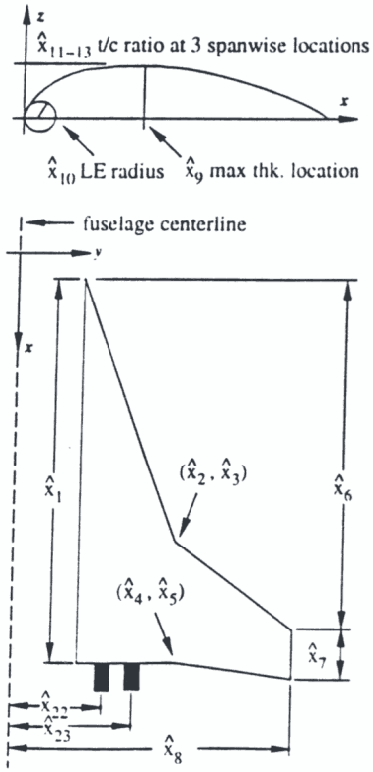

Fig. 2. Configuration design variables.

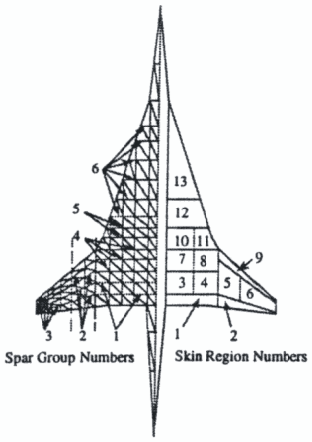

Fig. 3. Structural design variables.

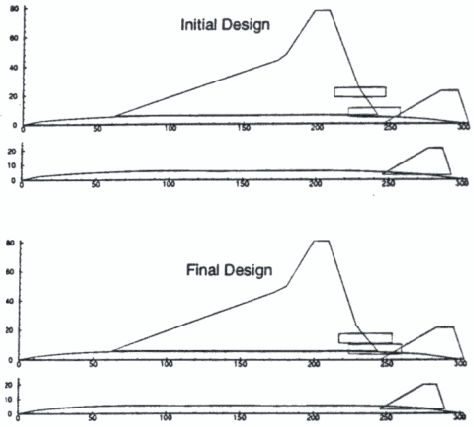

Fig. 5. Sample result.

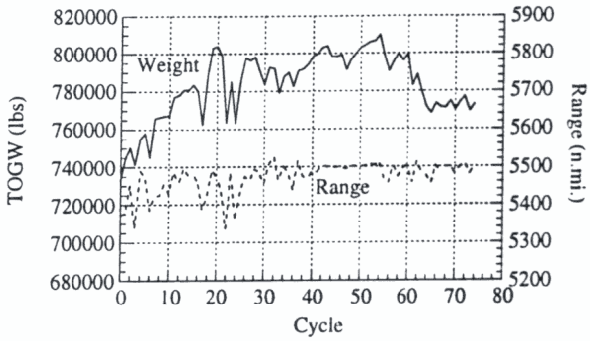

Fig. 6. Sample convergence plot.

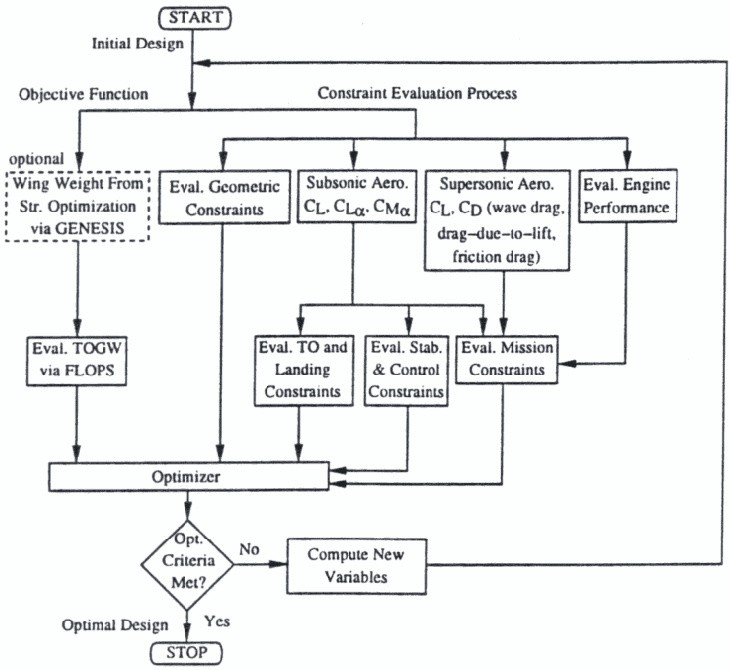

Fig. 4. MDO process for HSCT Design.

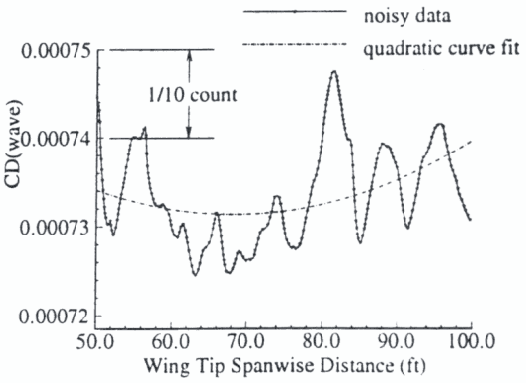

Fig. 7. Typical analysis noise.

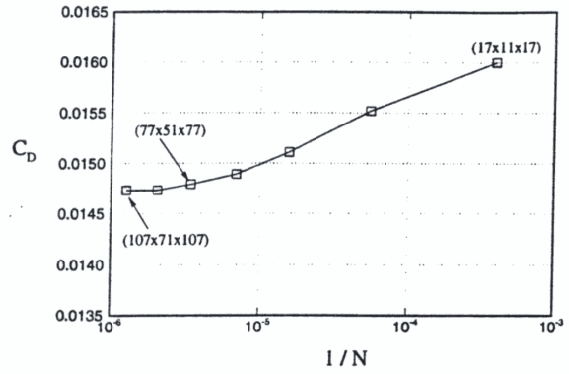

Fig. 8. Typical drag convergence - Euler.

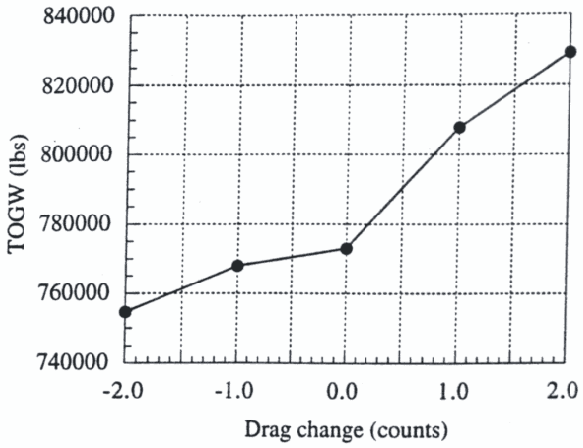

Fig. 11. TOGW sensitivity to drag errors.

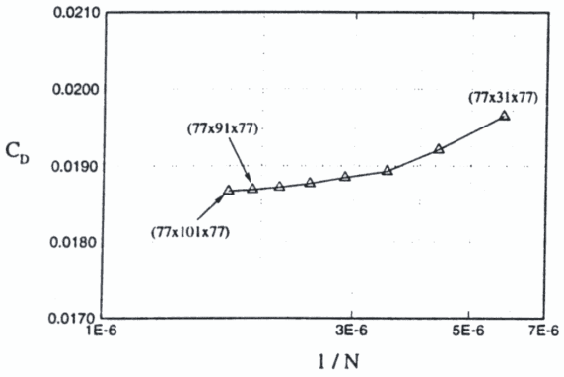

Fig. 9. Typical drag convergence - PNS.

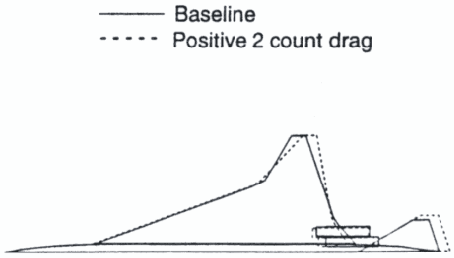

(a)

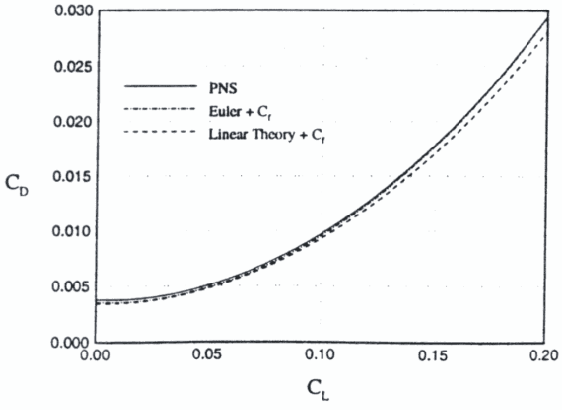

Fig. 10. Drag polar analysis comparison.

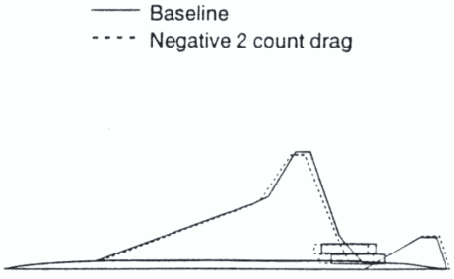

(b)

Fig. 12a,b. HSCT configuration sensitivity to drag errors.

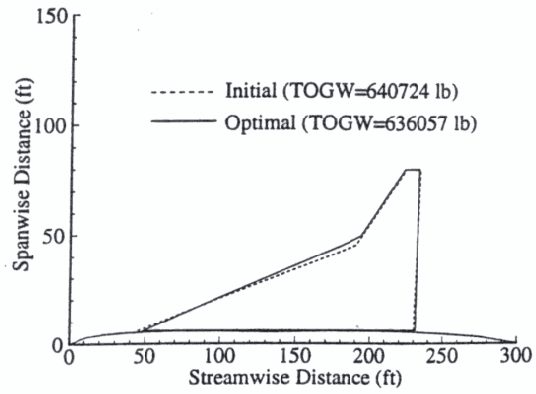

(a)

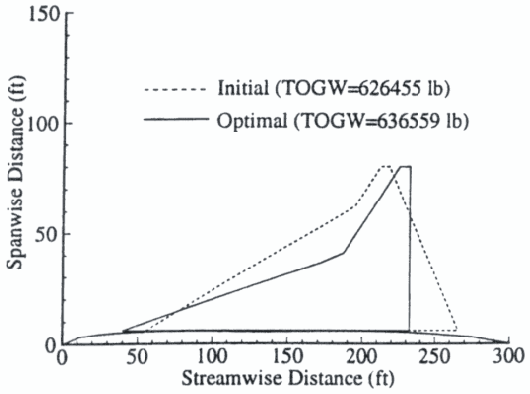

(b)

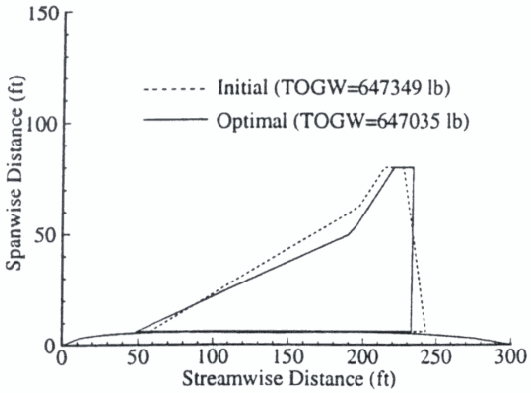

(c)

Fig. 13a,b,c. HSCT designs without response surface models.

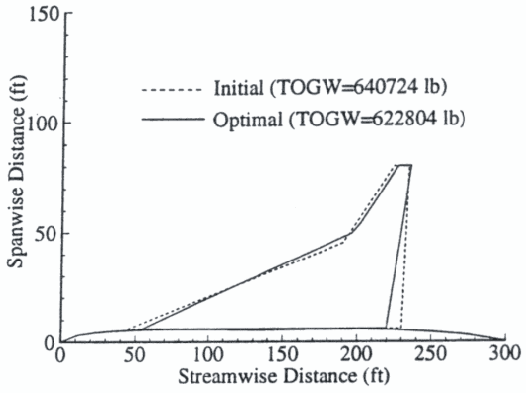

(a)

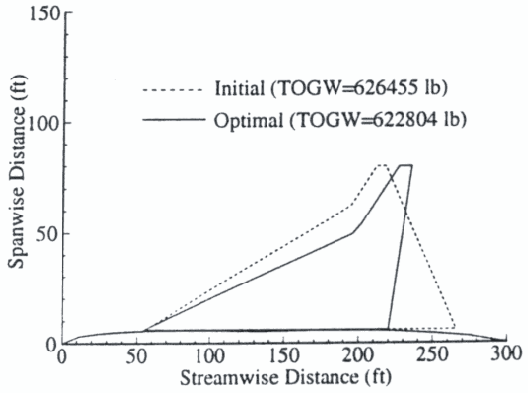

(b)

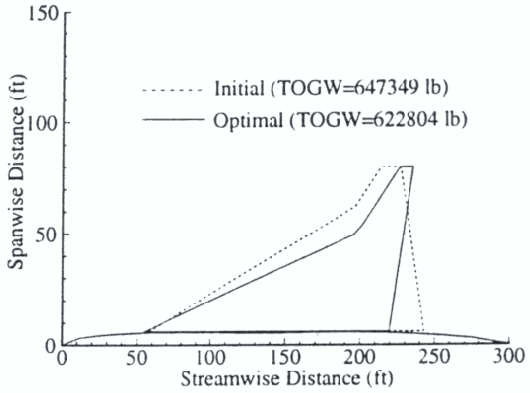

(c)

Fig. 14a,b,c. HSCT designs with response surface models.